

# Multifractal zone plates

Fernando Giménez,<sup>1</sup> Walter D. Furlan,<sup>2</sup> Arnau Calatayud,<sup>3</sup> and Juan A. Monsoriu<sup>3,\*</sup>

<sup>1</sup>*I.U. Matemática Pura y Aplicada, Universidad Politécnica de Valencia, E-46022 Valencia, Spain*

<sup>2</sup>*Departamento de Óptica, Universidad de Valencia, E-46100 Burjassot (Valencia), Spain*

<sup>3</sup>*Centro de Tecnologías Físicas, Universidad Politécnica de Valencia, E-46022 Valencia, Spain*

\*Corresponding author: [jmonsori@fis.upv.es](mailto:jmonsori@fis.upv.es)

Received April 14, 2010; revised June 13, 2010; accepted June 13, 2010;  
posted June 15, 2010 (Doc. ID 127031); published July 26, 2010

We present multifractal zone plates (MFZPs) as what is to our knowledge a new family of diffractive lenses whose structure is based on the combination of fractal zone plates (FZPs) of different orders. The typical result is a composite of two FZPs with the central one having a first-order focal length  $f$  surrounded by outer zones with a third-order focal length  $f$ . The focusing properties of different members of this family are examined and compared with conventional composite Fresnel zone plates. It is shown that MFZPs improve the axial resolution and also give better performance under polychromatic illumination. © 2010 Optical Society of America  
*OCIS codes:* 050.1940, 050.1970.

## 1. INTRODUCTION

Diffractive optical elements are most beneficial in many applications where they can perform tasks that are difficult, or even impossible, with conventional refractive optics because most solids are strongly absorbing in some spectral regions. Particularly, diffractive lenses, like Fresnel zone plates [1], can be used for focusing and imaging in terahertz tomography [2], soft x-ray microscopy [3,4], astronomy [5,6], and lithography [7].

As is well known, the conventional Fresnel zone plate consists of alternating transparent and opaque circular rings with the same area, so the transmittance of the lens is periodic along the square of the radial coordinate. The spatial resolution that can be achieved with these devices is of the order of the width of the outermost zone and is therefore limited by the smallest structure that can be fabricated by lithography [8,9]. In order to increase the resolution of these lenses several modified Fresnel zone plates have been proposed [10,11]. In particular, composite zone plates (CZPs) formed by a central zone plate with a first-order focal length  $f$ , surrounded by extra zones whose third-order focal length is also  $f$ , give an improved resolution and also increase the focused energy.

Photon sieves [4,5] are another kind of diffractive optical element, developed for focusing and imaging soft x rays with high resolution capabilities. A photon sieve is essentially a Fresnel zone plate where the clear zones are replaced with a great number of non-overlapping holes of different sizes. This configuration improves the diffraction efficiency of the lens and produces a sharp focal spot. However, it has been proved that the modified Fresnel zone plate can produce focal spots still better than those generated by photon sieves [11].

On the other hand, aside from conventional Fresnel zone plates, other geometries for two-dimensional photonic-image-forming structures have been proposed. To this category belong the fractal zone plates (FZPs) [12]. A FZP is characterized by its fractal profile along the

square of the radial coordinate. When illuminated by a parallel wavefront a FZP produces multiple foci, the main lobe of which coincides with those of the associated conventional zone plate (actually, under certain circumstances, a FZP can be thought as a conventional zone plate with certain missing zones), but the internal structure of each focus exhibits a characteristic fractal structure, reproducing the self-similarity of the originating FZP. FZPs have been successfully tested experimentally by different research groups working in diffractive optics [13–18] and they also inspired the invention of fractal optical devices for different applications [19–23].

In this paper we present multifractal zone plates (MFZPs) as a new family of diffractive lenses whose structure is basically a composite of two different FZPs. The focusing properties of different members of this family and their self-similar behavior are examined. The axial resolution of a MFZP is compared with the one corresponding to a FZP of the same focal length. Additionally, since most of applications of diffractive lenses are related with broadband illumination sources, the intensity distributions near the focus are evaluated by means of polychromatic merit functions and compared with those obtained with conventional CZPs.

## 2. MFZP DESIGN

Let us start revisiting the original proposal for the FZP [12]. It was based on the triadic Cantor set shown in the upper part of Fig. 1(a). The first step in the construction procedure consists of defining a straight-line segment of unit length called *initiator* (stage  $S=0$ ). Next, at stage  $S=1$ , the generator of the set is constructed by dividing the segment into three equal parts of length  $1/3$  and removing the central one. Following this procedure in subsequent stages  $S=2, 3, \dots$  it is easy to see that, in general, at stage  $S$  there are  $2^S$  segments (each one of length  $3^{-S}$ ) separated by  $2^{S-1}$  gaps. In Fig. 1(a), only the four first stages

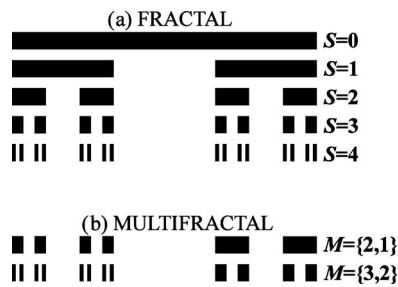


Fig. 1. (a) Triadic fractal Cantor set for the levels  $S=0, 1, 2, 3,$  and  $4$ . The structures for  $S=0$  and  $S=1$  are the initiator and generator, respectively. Note that the fractal set at stage  $S$  can be considered as a composite of two equivalent fractals at the previous stage  $S-1$ . (b) Multifractals as a composite of two different fractals.

are shown for clarity. Note that the Cantor set at a given stage  $S$  is constructed by two copies of the previous one,  $S-1$ , scaled to  $1/3$ , and located at the extremes of it. For example, the Cantor set  $S=4$  presents two scaled copies of the set  $S=3$ . According to this idea we can now define a *Cantor multifractal* of “multiorder”  $M=\{S_1, S_2\}$  to the composite of two different fractals of orders  $S_1$  and  $S_2$  scaled to  $1/3$  and located at the first and third parts of the structure, respectively. In this way, the conventional fractal  $S=4$  can be considered as a fractal composite  $M=\{3, 3\}$ . Figure 1(b) shows two examples of multifractals of multiorders  $M=\{2, 1\}$  and  $M=\{3, 2\}$ .

Assuming that Cantor multifractals can be mathematically represented by a one-dimensional binary function  $q(\varsigma)$  defined in the interval  $[0, 1]$ , MFZPs can be generated by performing a change of coordinates  $\varsigma=(r/a)^2$  and by rotating the transformed one-dimensional function around one of its extremes. The result is a zone plate having a radial coordinate  $r$  and an outermost ring of radius  $a$ . Figure 2(a) shows an example of a MFZP with  $M=\{3, 2\}$  and Fig. 2(b) shows a equivalent CZP with the same focal length and resolution. Note that a MFZP can be considered as a CZP but with some missing clear zones.

As we mentioned before, the resolution of zone plates is limited by the smaller zone width of the lens, which is limited by the manufacturing process. In order to increase the resolution of the lens, we will consider MFZPs,  $M=\{S_1, S_2\}$ , with  $S_2=S_1-1$ . Under this consideration, a MFZP is constructed with a central FZP with a principal focal length  $f=a^2/\lambda 3^{S_1}$  surrounded by a FZP whose third-order focal length is given by the same expression. With this configuration, the smaller zone of the outer FZP is 73.2% bigger than the smaller one of the central FZP.

### 3. AXIAL IRRADIANCE PROVIDED BY MFZP

Let us consider the irradiance at a given point on the optical axis, provided by a rotationally invariant pupil of radius  $a$  with an amplitude transmittance  $p(r)$ , illuminated by a monochromatic plane wave of wavelength  $\lambda$ . Within the Fresnel approximation, which is valid for most of the applications of interest (including x-ray microscopy [11]), this magnitude is given as a function of the axial distance from the pupil plane,  $z$ , as

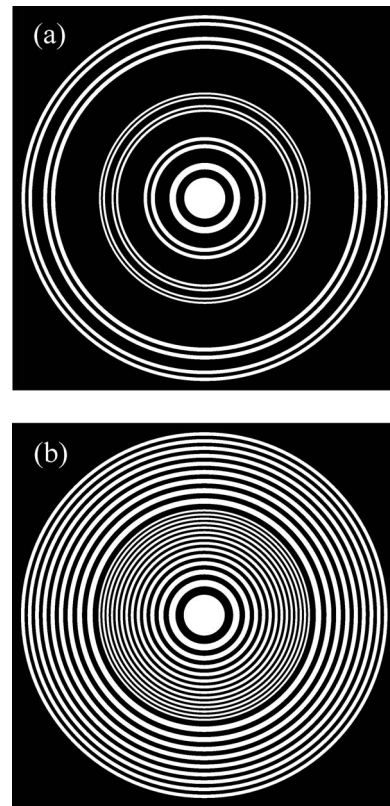


Fig. 2. (a) MFZP generated at  $M=\{3, 2\}$  and (b) the equivalent CZP.

$$I(z) = \left( \frac{2\pi}{\lambda z} \right)^2 \left| \int_0^a p(r_o) \exp\left(-i \frac{\pi}{\lambda z} r_o^2\right) r_o dr_o \right|^2. \quad (1)$$

If the pupil transmittance is defined in terms of the normalized variable  $\varsigma=(r/a)^2$ , the irradiance can be expressed as

$$I(u) = 4\pi^2 u^2 \left| \int_0^1 q(\varsigma) \exp(-i2\pi u \varsigma) d\varsigma \right|^2, \quad (2)$$

where  $q(\varsigma)=p(r_o)$  and  $u=a^2/2\lambda z$  is the reduced axial coordinate. Thus, the axial irradiance can be expressed in terms of the Fourier transform of the mapped pupil function  $q(\varsigma)$ . If the pupil function  $q(\varsigma)$  holds a fractal structure, from well-known properties of fractals, it is direct to conclude that such a system will provide an irradiance along the optical axis also with a self-similar profile.

Using Eq. (2), we have first computed the axial irradiances produced by the two zone plates that are necessary to construct a MFZP of multiorder  $M=\{3, 2\}$ . Figure 3(a) shows the axial irradiance produced by the central FZP of order  $S=3$  around the main focus located at a normalized distance  $u=3^S/2$ . Note that this central FZP can be also considered as a MFZP  $M=\{3, 0\}$ , where “0” indicates that the outer FZP has been removed. The axial response for this central FZP exhibits a single major focus and a number of subsidiary focal points surrounding it, producing a focus region with a characteristic fractal profile [12]. Figure 3(b) shows the irradiance produced by the outer FZP of order  $S=2$ . In this case there are three foci in the same axial range; these correspond to the first, third, and fifth

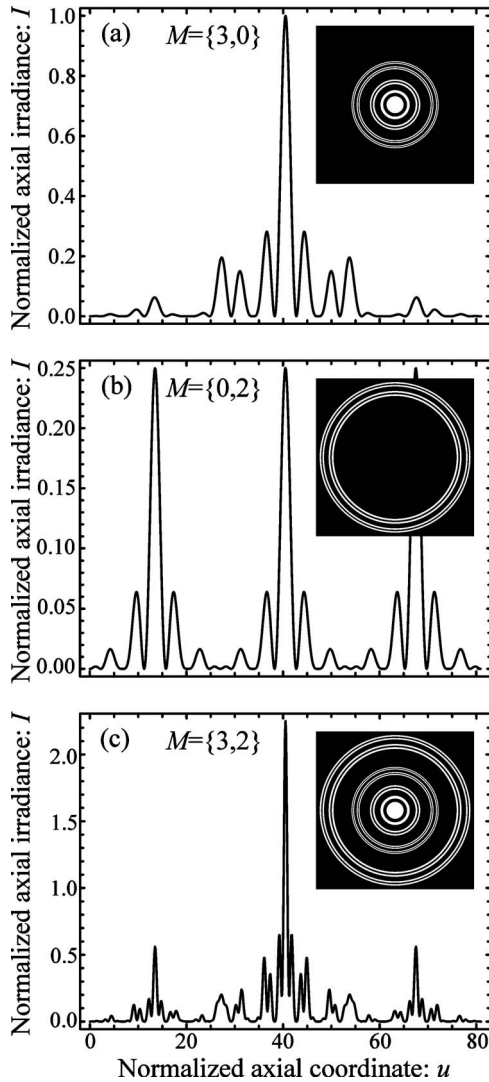


Fig. 3. Axial irradiances provided by different MFZPs shown in the inset. Note that in (c) {3,2} is the composite of {0,2} and {3,0}.

diffraction orders of the lens. However, compared with the previous case, the intensity at each focus has been reduced by 75%.

The axial irradiance for a MFZP of multiorder  $M = \{3,2\}$  is shown in Fig. 3(c) and obviously is the result of the interference between the fields diffracted by the central FZP of order  $S=3$  and the outer FZP of order  $S=2$ . Note that the composite of the two FZPs increases the focused energy and produces a tighter main focus, improving the axial resolution of the lens. This main focus of a MFZP is located at a normalized distance given by  $u_0 = 3^{\max(S_1, S_2)}/2$ , i.e.,  $u_0 = 3^{S_1}/2$  for  $S_2 = S_1 - 1$ .

Interestingly, MFZPs preserve the self-similarity property of the axial irradiance attributed to FZPs. To support this assertion, we have computed in Fig. 4 the axial irradiance produced by MFZPs of orders  $M = \{4,3\}$  and  $M = \{3,2\}$  around their main foci. It can be seen that the axial intensity distribution corresponding to MFZPs of low level forms the envelope of the curves of the upper ones. We have found that the same behavior is also observed in general for MFZPs,  $M = \{S_1, S_2\}$ , with  $S_2 < S_1 - 1$ . In these cases the main focus of the central FZP is co-

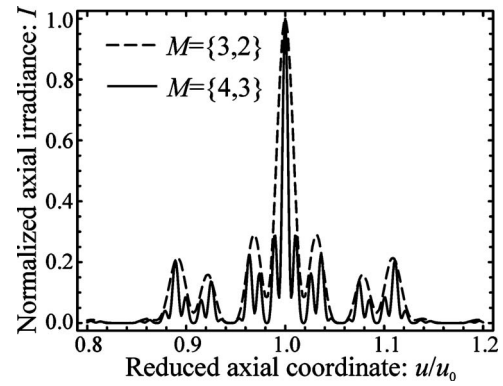


Fig. 4. Self-similar behavior of the axial irradiances provided by two MFZPs around the corresponding main focus.

incident with the  $N$ -order focus of the outer FZP, provided that  $S_2 = S_1 - (N-1)/2$ , where  $N$  is an odd integer number.

On the other hand, when polychromatic light is employed, the multiple subsidiary foci around the main focus of a MFZP overlap for different wavelengths creating an overall extended depth of focus, which should be less sensitive to the chromatic aberration than the equivalent CZP. Next, we analyze this hypothesis.

The behavior of a MFZP under broadband illumination is evaluated here following the conventional approach, in terms of the tristimuli values [24], computed along the optical axis,

$$\begin{aligned} X &= \int_{\lambda_2}^{\lambda_1} I(r=0, z; \lambda) S(\lambda) \bar{x} d\lambda, \\ Y &= \int_{\lambda_2}^{\lambda_1} I(r=0, z; \lambda) S(\lambda) \bar{y} d\lambda, \\ Z &= \int_{\lambda_2}^{\lambda_1} I(r=0, z; \lambda) S(\lambda) \bar{z} d\lambda, \end{aligned} \quad (3)$$

where  $S(\lambda)$  is the spectral distribution of the source,  $(\bar{x}, \bar{y}, \bar{z})$  are the three sensitivity chromatic functions of the detector, and  $(\lambda_1, \lambda_2)$  represent the considered wavelength interval. In particular, in the assessment of visual systems  $(\bar{x}, \bar{y}, \bar{z})$  are usually the sensitivity functions of the human eye (CIE 1931) and the axial response is normally expressed in terms of the axial illuminance  $Y$  and the axial chromaticity coordinates  $x, y$ ,

$$x = \frac{X}{X+Y+Z}, \quad y = \frac{Y}{X+Y+Z}. \quad (4)$$

To evaluate the performance of a MFZP under polychromatic illumination we have computed Eqs. (3) and (4) for the zone plates shown in Fig. 2. We numerically computed 41 monochromatic irradiances for equally spaced wavelengths ranging from 380 to 780 nm. The standard illuminant  $C$  was used as a spectral distribution of the source. The result is shown in Fig. 5. Clearly, the axial illuminance for the MFZP has an increased depth of focus as compared with the conventional CZP [Fig. 5(a)]. The degree of achromatization is evident in the display of the chromaticity [Fig. 5(b)]. In this figure we have computed

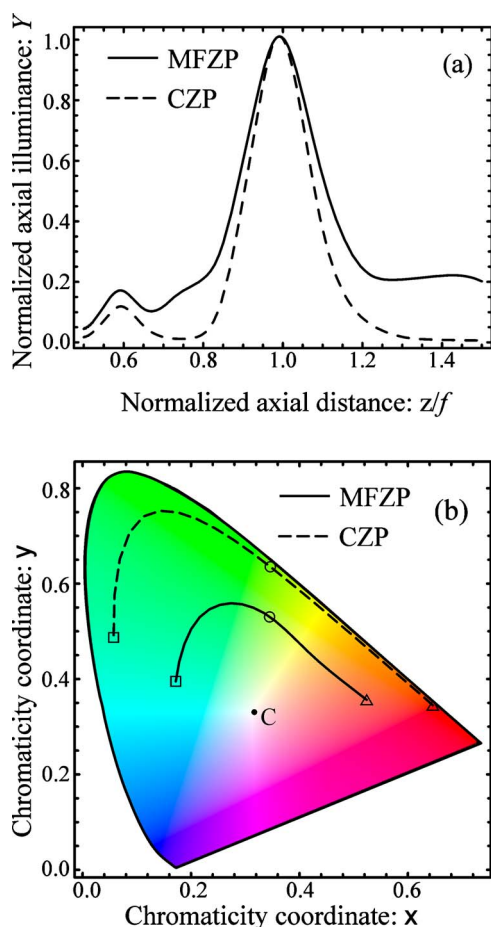


Fig. 5. (Color online) (a) Polychromatic axial illuminance computed for the zone plates in Fig. 2. The chromaticity of both curves is shown in (b); the continuous line corresponds to the MFZP and the dashed line corresponds to the CZP.

the chromaticity for the axial points around the main focus:  $0.9 < z/f < 1.1$ . The triangles and squares represent  $z/f=0.9$  and  $z/f=1.1$ , respectively, while the circles represent  $z=f$  for the design wavelength. It can be observed that the MFZP exhibits a “slow” axial chromaticity variation than the CZP and also that almost the whole curve for this lens is closer to the point representing the white illuminant.

#### 4. CONCLUSIONS

Multifractal zone plates (MFZPs) based on Cantor multifractal sets have been proposed. The focusing properties of MFZPs have been numerically evaluated and the self-similarity of the axial irradiances is verified. As these lenses can be considered as composites of two FZPs, they combine the advantages of fractal and composite diffractive lenses. It has been shown that the composite of a central FZP of focal length  $f$  with an outer FZP with the same third-order focal length gives an increased axial resolution and also an increase in the focused energy with respect to a single FZP. Additionally, MFZPs produce a series of fractal multiple foci that are useful when dealing with broadband sources. In fact, it has been also shown that in these situations, MFZPs provide an increase in the depth of focus and a reduction in the chromaticity dis-

tribution in comparison with the equivalent CZP. Moreover, the transverse resolution of both kinds of zone plates is nearly the same as occurs for non-composite FZPs [17,22]. The potential applications of MFZPs are numerous in the entire electromagnetic spectrum, mainly for applications in which the illumination sources are wideband and require a high depth of field, as in the case of x-ray microscopy.

#### ACKNOWLEDGMENTS

We acknowledge the financial support from Grants DPI2008-02953 and TRA2009-0215, Ministerio de Ciencia e Innovación, Spain. We also acknowledge the support from Generalitat Valenciana, Spain (PROMETEO2009-077 and ACOMP/2010/052) and from Universidad Politécnica de Valencia, Spain (PAID-05-09 and PAID-06-08).

#### REFERENCES

1. J. Ojeda-Castañeda and C. Gómez-Reino, eds., *Selected Papers on Zone Plates* (SPIE Optical Engineering, 1996).
2. S. Wang and X. Zhang, “Terahertz tomographic imaging with a Fresnel lens,” *Opt. Photonics News* **13**, 59 (2002).
3. Y. Wang, W. Yun, and C. Jacobsen, “Achromatic Fresnel optics for wideband extreme-ultraviolet and X-ray imaging,” *Nature* **424**, 50–53 (2003).
4. L. Kipp, M. Skibowski, R. L. Johnson, R. Berndt, R. Adlung, S. Harm, and R. Seemann, “Sharper images by focusing soft x-rays with photon sieves,” *Nature* **414**, 184–188 (2001).
5. G. Andersen, “Large optical photon sieve,” *Opt. Lett.* **30**, 2976–2978 (2005).
6. R. Hyde, “Eyeglass. 1. Very large aperture diffractive telescopes,” *Appl. Opt.* **38**, 4198–4212 (1999).
7. R. Menon, D. Gil, G. Barbastathis, and H. Smith, “Photon sieve lithography,” *J. Opt. Soc. Am. A* **22**, 342–345 (2005).
8. E. H. Anderson, V. Boegli, and L. P. Muray, “Electron beam lithography digital pattern generator and electronics for generalized curvilinear structures,” *J. Vac. Sci. Technol. B* **13**, 2529–2534 (1995).
9. E. H. Anderson, D. L. Olynick, B. Harteneck, E. Veklerov, G. Denbeaux, W. Chao, A. Lucero, L. Johnson, and D. Atwood, “Nanofabrication and diffractive optics for high resolution x-ray applications,” *J. Vac. Sci. Technol. B* **18**, 2970–2975 (2000).
10. M. J. Simpson and A. G. Michette, “Imaging properties of modified Fresnel zone plates,” *Opt. Acta* **31**, 403–413 (1984).
11. Q. Cao and J. Jahns, “Modified Fresnel zone plates that produce sharp Gaussian focal spots,” *J. Opt. Soc. Am. A* **20**, 1576–1581 (2003).
12. G. Saavedra, W. D. Furlan, and J. A. Monsoriu, “Fractal zone plates,” *Opt. Lett.* **28**, 971–973 (2003).
13. J. A. Davis, L. Ramirez, J. A. Rodrigo Martín-Romo, T. Alieva, and M. L. Calvo, “Focusing properties of fractal zone plates: experimental implementation with a liquid-crystal display,” *Opt. Lett.* **29**, 1321–1323 (2004).
14. H.-T. Dai, X. Wang, and K.-S. Xu, “Focusing properties of fractal zone plates with variable lacunarity: experimental studies based on liquid crystal on silicon,” *Chin. Phys. Lett.* **22**, 2851–2854 (2005).
15. Y. J. Liu, H. T. Dai, X. W. Sun, and T. J. Huang, “Electrically switchable phase-type fractal zone plates and fractal photon sieves,” *Opt. Express* **17**, 12418–12423 (2009).
16. S. H. Tao, X.-C. Yuan, J. Lin, and R. Burge, “Sequence of focused optical vortices generated by a spiral fractal zone plates,” *Appl. Phys. Lett.* **89**, 031105 (2006).
17. W. D. Furlan, G. Saavedra, and J. A. Monsoriu, “White-light imaging with fractal zone plates,” *Opt. Lett.* **32**, 2109–2111 (2007).

18. D. Wu, L.-G. Niu, Q.-D. Chen, R. Wan, and H.-B. Sun, "High efficiency multilevel phase-type fractal zone plates," *Opt. Lett.* **33**, 2913–2915 (2008).
19. J. A. Monsoriu, G. Saavedra, and W. D. Furlan, "Fractal zone plates with variable lacunarity," *Opt. Express* **12**, 4227–4234 (2004).
20. F. Giménez, J. A. Monsoriu, W. D. Furlan, and A. Pons, "Fractal photon sieves," *Opt. Express* **14**, 11958–11963 (2006).
21. J. A. Monsoriu, W. D. Furlan, G. Saavedra, and F. Giménez, "Devil's lenses," *Opt. Express* **15**, 13858–13864 (2007).
22. O. Mendoza-Yero, M. Fernández-Alonso, G. Mínguez-Vega, J. Lácis, V. Climent, and J. A. Monsoriu, "Fractal generalized zone plates," *J. Opt. Soc. Am. A* **26**, 1161–1166 (2009).
23. W. D. Furlan, F. Giménez, A. Calatayud, and J. A. Monsoriu, "Devil's vortex-lenses," *Opt. Express* **17**, 21891–21896 (2009).
24. M. J. Yzuel and J. Santamaria, "Polychromatic optical image. Diffraction limited system and influence of the longitudinal chromatic aberration," *Opt. Acta* **22**, 673–690 (1975).